electronic reprint

Journal of
Applied Crystallography
ISSN 0021-8898
Editor: **Anke R. Pyzalla**

Critical opalescence points to thermodynamic instability: relevance to small-angle X-ray scattering of resorcinol–formaldehyde gel formation at low pH

Cedric J. Gommes, Nathalie Job, Jean-Paul Pirard, Silvia Blacher and Bart Goderis

J. Appl. Cryst. (2008). **41**, 663–668

Copyright © International Union of Crystallography

Author(s) of this paper may load this reprint on their own web site or institutional repository provided that this cover page is retained. Republication of this article or its storage in electronic databases other than as specified above is not permitted without prior permission in writing from the IUCr.

For further information see http://journals.iucr.org/services/authorrights.html

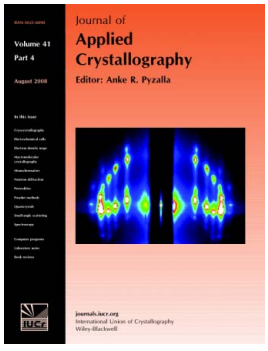

Many research topics in condensed matter research, materials science and the life sciences make use of crystallographic methods to study crystalline and non-crystalline matter with neutrons, X-rays and electrons. Articles published in the *Journal of Applied Crystallography* focus on these methods and their use in identifying structural and diffusion-controlled phase transformations, structure–property relationships, structural changes of defects, interfaces and surfaces, *etc.* Developments of instrumentation and crystallographic apparatus, theory and interpretation, numerical analysis and other related subjects are also covered. The journal is the primary place where crystallographic computer program information is published.

Crystallography Journals Online is available from **journals.iucr.org**

Journal of
Applied Crystallography
ISSN 0021-8898

Received 6 October 2007
Accepted 17 May 2008

Critical opalescence points to thermodynamic instability: relevance to small-angle X-ray scattering of resorcinol–formaldehyde gel formation at low pH

Cedric J. Gommes,[a]* Nathalie Job,[a] Jean-Paul Pirard,[a] Silvia Blacher[a] and Bart Goderis[b]

[a]Department of Chemical Engineering, University of Liège, Institut de Chimie B6a, B-4000 Sart-Tilman Liège, Belgium, and [b]Chemistry Department, Catholic University of Leuven, Celestijnenlaan 200F, B-3001 Heverlee, Belgium. Correspondence e-mail: cedric.gommes@ulg.ac.be

During the formation at low pH of resorcinol–formaldehyde gels with a structure in the micrometre range, small-angle X-ray scattering exhibits a non-monotonic intensity variation as a function of reaction time. The data are analyzed in terms of scattering by statistical fluctuations of polymer concentration, the amplitude of which is maximal close to the critical point for phase separation between polymer and solvent. The data do not carry any morphological information, but they unambiguously show that the driving force of the gel formation is a thermodynamic instability of the polymerizing solution.

© 2008 International Union of Crystallography
Printed in Singapore – all rights reserved

1. Introduction

Resorcinol–formaldehyde (RF) aerogels and xerogels are organic porous materials that are synthesized *via* the hydrolysis and condensation of the precursor molecules in solution (Al-Muhtaseb & Ritter, 2003) in much the same way as inorganic sol-gel materials (Brinker & Scherer, 1990). Since the early work of Pekala (1989), these porous materials have received growing attention, notably as a result of their potential applications as adsorbents, thermal insulators, catalyst supports, fuel cell electrodes *etc.*

The microstructure of RF gels can be tailored to yield materials with pore size ranging from a few nanometres when the synthesis is performed at high pH to a few micrometres at low pH (Al-Muhtaseb & Ritter, 2003). Although much work has focused on the synthesis of RF materials with morphologies apt to fit specific applications, the physicochemical mechanisms that control the formation of their microstructure are still unclear. In the 1990s, Pekala & Schaefer (1993), and later Schaefer *et al.* (1995), suggested that the origin of porosity in RF gels at high pH be a microphase separation process triggered by the polymerization of the precursor molecules (see *e.g.* de Gennes, 1979). Many researchers, however, discuss the structuring of RF gels in terms of the same colloid aggregation mechanism as in inorganic sol-gel (*e.g.* Yamamoto *et al.*, 2001). It has recently been shown that *in situ* small-angle X-ray scattering (SAXS) does not enable discrimination between the two mechanisms (Gommes & Roberts, 2008). In comparison, low-pH RF gels have received far less attention. It is implicitly admitted by many authors (*e.g.* Al-Muhtaseb & Ritter, 2003) that their formation mechanism is not qualitatively different from that of high-pH gels.

The present paper reports *in situ* SAXS measurements performed during the formation of low-pH RF gels. Although the final gels have a structure in the micrometre range, an intense SAXS signal is observed in the course of the gel formation, which is analyzed in terms of X-ray scattering by concentration fluctuations.

2. Experimental

2.1. Resorcinol–formaldehyde gelling solutions

Resorcinol–formaldehyde aqueous solutions were prepared at three different pH values in the low-pH range (Job *et al.*, 2004). The resorcinol–formaldehyde molar ratio, R/F, and the dilution ratio, D, *i.e.* the solvent/$(R + F)$ molar ratio, were fixed at 0.5 (considered as the stoichiometric ratio) and 5.7, respectively. The total amount of solvent takes into account the deionized water added and the water and methanol (stabilizer) included in the formaldehyde solution.

Resorcinol (VWR International, 99%, 4.955 g) was first mixed with 9.4 ml of deionized water in 100 ml sealable flasks under magnetic stirring. The formaldehyde solution (Aldrich,

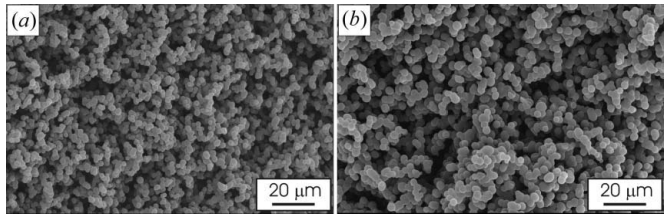

Figure 1
Scanning electron micrographs of resorcinol–formaldehyde xerogels synthesized at (*a*) pH = 2.0 and (*b*) pH = 3.0.

electronic reprint

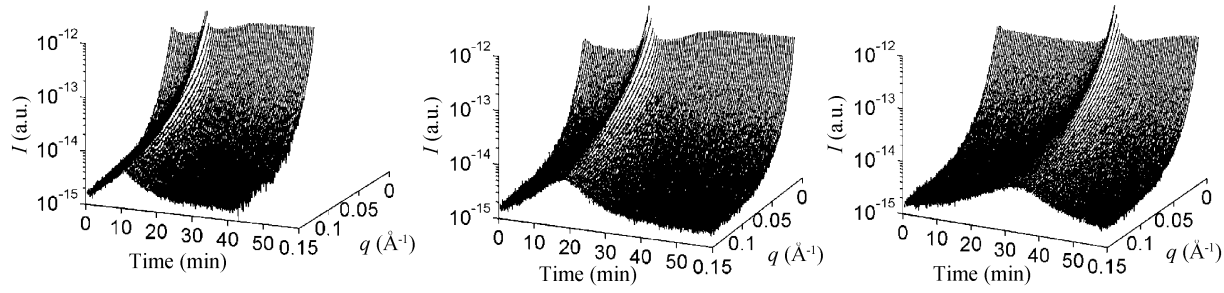

Figure 2
Time-resolved small-angle X-ray scattering patterns during the formation of resorcinol–formaldehyde gels at 343 K with (*a*) pH = 2.7, (*b*) pH = 3.0 and (*c*) pH = 3.7.

37 wt% in water, stabilized by 10–15 wt% methanol) was poured into a separated flask. All the solutions were then placed in a thermostat at 343 K. After temperature stabilization, the formaldehyde solution (6.75 ml) was added to the resorcinol solution. A first sample was prepared without any other additive. Two additional gels were synthesized at lower pH by adding concentrated HNO_3 (Aldrich, 69 wt% in water). The starting pH values were measured at 298 K on non-heated solution replicas (pH = 3.7, 3.0 and 2.7, respectively).

In the course of the reaction the solutions become turbid, which results from the formation of structures with a size comparable to the visible light wavelength (*e.g.* Tanaka, 1981). The solid phase of the final gels, after drying, is made up of aggregates of spherical objects of about 5 µm across, as shown in the scanning electron micrographs of Fig. 1. Nitrogen adsorption measurements further show that the spherical objects seen in the micrographs are non-porous (Job *et al.*, 2004).

2.2. Small-angle X-ray scattering

Time-resolved SAXS measurements were performed during the polymerization of the RF solutions at the Dutch–Flemish SRG beamline (BM26B) at the European Synchrotron Radiation Facility in Grenoble, France. Immediately after its preparation, a small fraction of the reacting solution was placed in a 1.5 mm-thick cell with a temperature control (343 K). Pinhole SAXS patterns were measured over time spans of 30 s on a two-dimensional CCD detector placed 3.5 m from the sample.

The isotropic SAXS data were rotationally averaged and expressed as the intensity as a function of the scattering vector modulus $q = (4\pi/\lambda)\sin(\theta/2)$, λ being the wavelength and θ the scattering angle. The intensity scattered by the empty sample holder was subtracted from the data. A correction was made for the detector response, and the data were normalized to the intensity of the primary beam measured by an ionization chamber placed downstream from the sample. The measured q range spans from 0.01 to 0.2 Å^{-1}, which roughly corresponds to length scales ranging from $2\pi/q \simeq 30$ Å to 600 Å.

3. Results

Fig. 2 represents on a semi-logarithmic scale the evolution of the scattering patterns of RF solutions at pH = 2.7, 3.0 and 3.7 as a function of reaction time. For all three solutions, the scattered intensity at any angle passes through a well defined maximum at an intermediate reaction time. The time for the maximum is approximately the same for all scattering angles. When increasing the pH from 2.7 to 3.7 the occurrence of the maximum shifts towards larger reaction times, from 10 to 35 min.

In order to explain the mechanism underlying these general features of SAXS, we refer to the patterns at early, intermediate and late reaction times of the solution at pH 3.7 as displayed in Fig. 3. This particular sample was used because it has the slowest kinetics, which eases the analysis of the processes at the various stages.

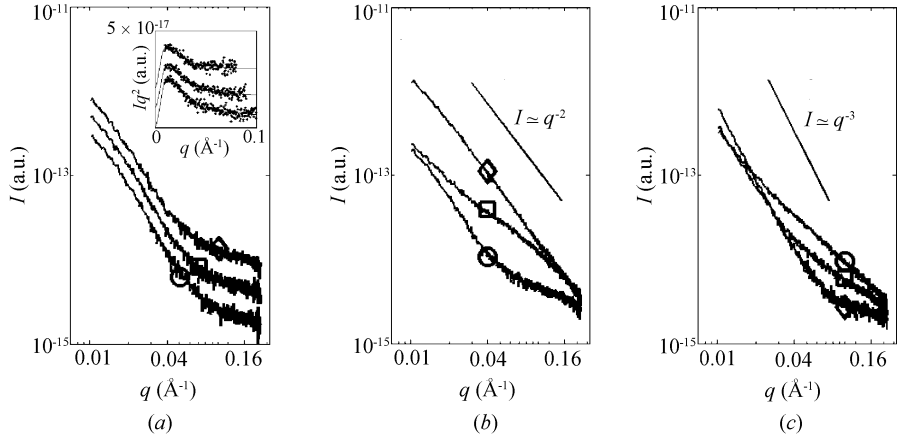

Figure 3
Small-angle X-ray scattering patterns of a resorcinol–formaldehyde sample with pH = 3.7, at (*a*) early reaction times t = 0 min (open circle), t = 8 min (open square), t = 15 min (open diamond); (*b*) intermediate reaction times t = 20 min (circle), t = 30 min (square), t = 35 min (diamond); and (*c*) late reaction times t = 40 min (circle), t = 45 min (square), t = 60 min (diamond). In (*a*), the data are arbitrarily shifted vertically; the Kratky plots of the same data are in the inset, in which the solid lines are fits of a model of branched polymers (see Gommes, Goderis, Pirard & Blacher, 2007).

electronic reprint

At early reaction times [$t < 15$ min; Fig. 3(*a*)], SAXS exhibits decay at low angles with a slight curvature, with a flat background at larger angles. When Kratky–Porod plots are drawn from these data [inset of Fig. 3(*a*)], a maximum appears in the curves which is typical of branched polymers in solution (Burchard, 1977; Glatter & Kratky, 1982). The scattering data are in agreement with a model of branched polymers (Burchard, 1977; Gommes, Goderis, Pirard & Blacher, 2007), as displayed in the inset of Fig. 3(*a*). The fit shows that the position of the maximum shifts slightly towards smaller angles, which corresponds to an increase of the radius of gyration of the polymers with time.

At intermediate reaction times [$20 < t < 35$ min; Fig. 3(*b*)], the scattered intensity at all angles increases by almost an order of magnitude. At $t = 20$ min, the SAXS pattern is similar to those of Fig. 3(*a*), *i.e.* of branched polymers in solution. At $t = 30$ min, a power-law scattering with exponent -2 appears at large angles, and this progressively expands over the entire measured range of q at $t = 35$ min.

At long reaction times [$t > 40$ min; Fig. 3(*c*)], the q^{-2} scattering progressively vanishes; a power-law scattering with exponent -3 develops at small angles and a plateau, characteristic of a featureless structure, appears at large angles. At the end of the process, the q^{-2} scattering has completely disappeared.

4. Discussion

4.1. Polymerization-induced critical opalescence

The most striking feature of the measured SAXS data is a tenfold temporary increase of the scattered intensity with exponent -2 at intermediate reaction times. In the context of a polymerizing solution, the exponent -2 could *a priori* be analyzed in terms of the asymptotic exponent of a branched polymer structure (Glatter & Kratky, 1982). In this case, the increase of the intensity would be analyzed in terms of the aggregation of oligomers in a type of cluster–cluster aggregation. If this were the case, the scattered intensity I would scale in the asymptotic range as $I \simeq cv^2(qL)^{-2}$, with c the concentration of polymers, v their volume and L their linear size. In this particular context, the exponent 2 is a fractal dimension, so that the volume would scale like $v \simeq L^2$, which would finally lead to $I \simeq cvq^{-2}$. As mass conservation requires that the product cv be constant, the growth of polymer structures cannot be responsible for the observed increase of the SAXS signal. Furthermore, with that particular analysis, the subsequent lowering of the SAXS intensity would also be difficult to understand.

All the features of the present SAXS data can be understood as a critical opalescence phenomenon. Critical opalescence is classically explained in terms of water vapor being compressed (Stanley, 1971). At pressures much lower than the dew point, the vapor is transparent because it is homogeneous over distances comparable to the visible light wavelength. When the pressure is increased to close to the dew point, statistical density fluctuations appear with a broad range of characteristic lengths. The fluctuations in the micrometre range scatter the visible light, which renders the system turbid (opalescent). When the dew point is reached and exceeded, phase separation occurs: water droplets are formed and the fluctuations in the remaining vapor disappear. As the droplets are significantly larger than the visible light wavelength, the system is transparent again. Therefore, critical opalescence leads to a temporary increase of the scattered intensity, and the scattering by fluctuations obeys a power law of the angle with exponent -2 (Stanley, 1971; An *et al.*, 1999).

In the present context, the motor of the phase separation and of the critical fluctuations is the polymerization itself. Polymerization-induced phase separation is quite common in polymer blends (Olabisi *et al.*, 1979; Nakanishi, 1997; Ishii & Ryan, 2000; Goossens *et al.*, 2006) as well as in gelling solutions (Pekala & Schaefer, 1993; Sefcik & McCormick, 1997; Gommes, Goderis & Pirard, 2007; Serrano Aroca *et al.*, 2007). The solubility of a polymer in a solvent, or in another polymer, is a decreasing function of its degree of polymerization N (de Gennes, 1979; Olabisi *et al.*, 1979). A polymerization reaction can therefore destabilize an initially homogeneous solution and make it demix into polymer-rich and solvent-rich phases. When approaching the critical degree of polymerization, statistical concentration fluctuations at all wavelengths increase in amplitude, which leads to an increase of the scattered intensity. When phase separation occurs, the polymer concentration in the solvent-rich phase progressively decreases and so does the amplitude of the concentration fluctuations.

To check the hypothesis of critical opalescence, the SAXS data are analyzed quantitatively in the following section in terms of the Ornstein–Zernicke–Debye theory (Stanley, 1971), which enables us to estimate the critical exponents and compare them with theoretical values.

4.2. Orstein–Zernicke–Debye fits and critical exponents

The SAXS data are hereafter analyzed in terms of scattering by fluctuations, according to the Ornstein–Zernicke–Debye theory. The SAXS data are fitted with the function (An *et al.*, 1999)

$$I(q) = C\chi/(1 + \xi^2 q^2), \tag{1}$$

where C is a constant related notably to the volume fraction of the polymer and to the concentration dependence of the electron density, χ is the osmotic compressibility of the polymers, and ξ is a correlation length.

To fit the data with equation (1), $1/I(q)$ is plotted against q^2 and a linear fit is performed, as illustrated in Fig. 4 for the sample at pH = 3.0. Although the data are noisy, the lower part of Fig. 4 shows that the experimental points are uniformly distributed above and below the fitted line. From the slope and intercept of the fitted line, the correlation length ξ and the product $C\chi$ are estimated, together with their statistical uncertainty. The quantity $C\chi$ is referred to as I_0 hereafter. It has to be stressed that I_0 is truly proportional to χ because all factors that enter the unknown constant C remain unchanged

electronic reprint

while the reaction proceeds; they are also the same for all samples.

Fig. 5 illustrates the evolution of ξ and of I_0 as a function of reaction time for the sample prepared at pH = 3.0. Both ξ and I_0 (and therefore χ) diverge at a critical time t_c. The insets plot the same data on double logarithmic scales, before and after the critical time. They show that the evolutions of ξ and of I_0 do not follow a power law of the time, either before or after t_c. Fig. 6 plots the values of I_0 (proportional to χ) as a function of ξ, independently of the reaction time. For all three samples, the points fall on a curve that is slightly curvilinear at low values of ξ. At large values of ξ, the curves are well approximated by power laws: $\chi \simeq \xi^{1.9\ (0.1)}$ before the critical point and $\chi \simeq \xi^{2.0\ (0.1)}$ after the critical point.

Critical phenomena are described by power laws with specific exponents (Stanley, 1971). Generally, close to a critical point the properties of a system scale with $\varepsilon = (T - T_c)/T_c$, where T is the temperature and T_c is the critical temperature; in the case of polymeric systems the properties also scale with the degree of polymerization N (de Gennes, 1979):

$$\chi \simeq N^{g}\varepsilon^{-\gamma} \quad \text{and} \quad \xi \simeq N^{n}\varepsilon^{-\upsilon}. \tag{2}$$

The classical values for the latter parameters are $g = 0$, $\gamma = 1$, $n = \frac{1}{4}$ and $\upsilon = \frac{1}{2}$ (Sanchez, 1989). In the present case T is constant, and the system is brought into a critical state by an increase of T_c. In the context of the Flory–Huggins theory, the critical temperature is predicted to depend on the degree of polymerization *via* (Billmeyer, 1984)

$$\frac{1}{T_c} = \frac{1}{\Theta}\left(1 + \frac{C_1}{N^{1/2}}\right), \tag{3}$$

where C_1 is a constant and Θ is the limit of the critical temperature for an infinite degree of polymerization. For appropriate values of Θ and C_1, increasing N leads to an increase of T_c above the reaction temperature T, which triggers a phase separation.

As the relationship between ε and N is not linear [equation (3)], and as the kinetics of polymerization does not necessarily follow a power law of the time, neither ξ nor χ is expected to evolve as a power law of the time; this behavior is also seen in the insets of Fig. 5. At any state of the polymerization, however, χ and ξ are related to each other by a power law. It has indeed to be noted that the critical point for phase

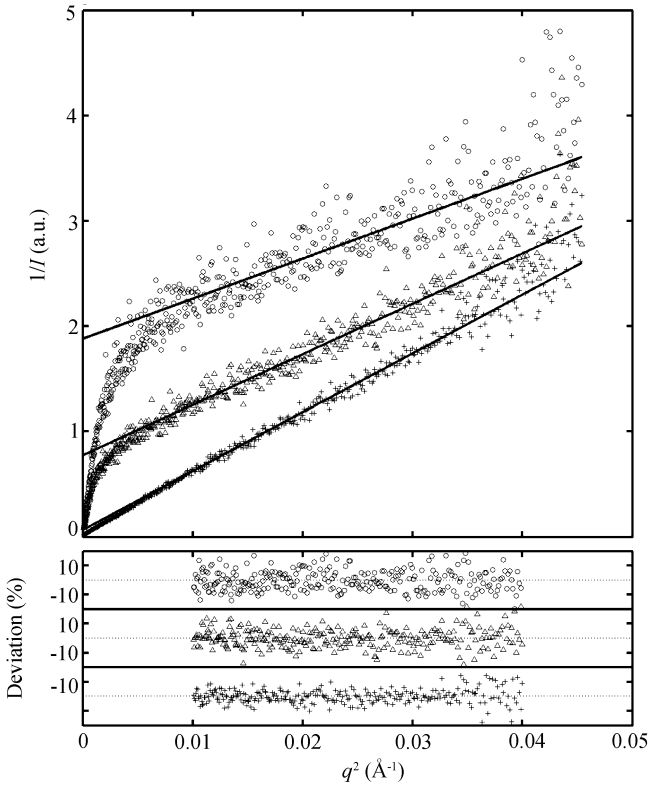

Figure 4
Ornstein–Zernicke–Debye plots, with the corresponding linear fits (top) and relative deviations between the fits and the data in the range where the fits are performed (bottom); sample synthesized with pH = 3.0, at t = 10 min (circles), t = 13 min (triangles) and t = 18 min (plus signs).

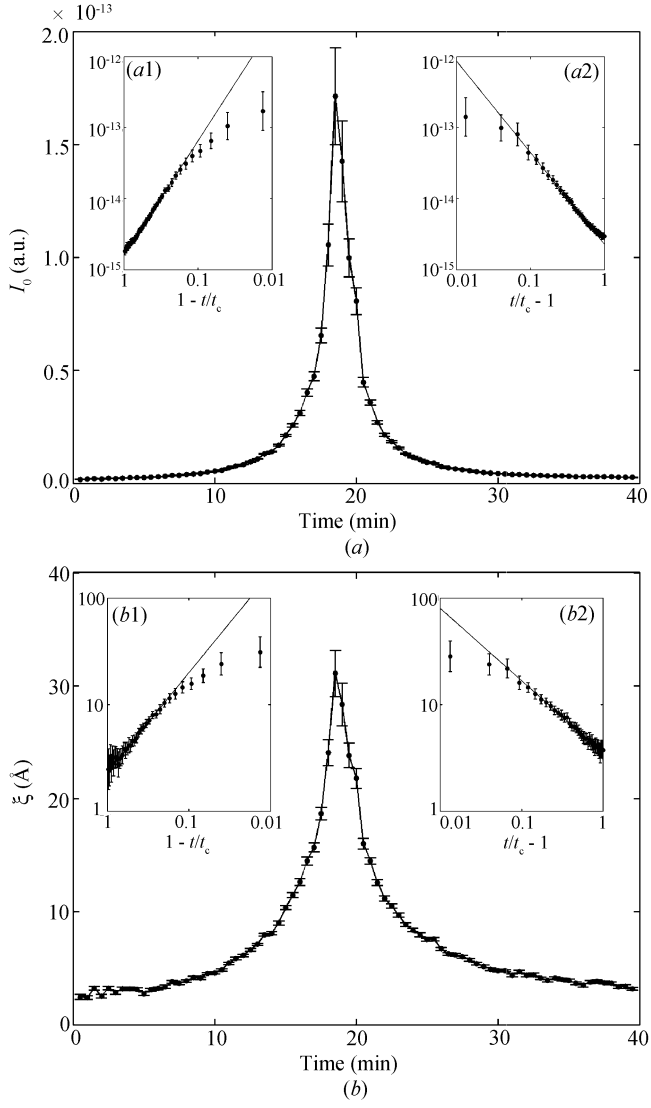

Figure 5
Time evolution (*a*) of I_0 (proportional to the osmotic compressibility χ) and (*b*) of the correlation length ξ for the sample synthesized at pH = 3.0. The insets show the same data on double logarithmic scales, before (*a*1 and *b*1) and after (*a*2 and *b*2) the critical point.

electronic reprint

separation is generally reached for a finite degree of polymerization N [equation (3)]. Therefore, close to the critical point, the dependence of ξ and χ in equation (2) is dominated by ε, and the relation between χ and ξ is

$$\chi \simeq \xi^{\gamma/\upsilon}, \tag{4}$$

with $\gamma/\nu = 2$, according to the classical theory (Sanchez, 1989). The latter value is in remarkable agreement with that obtained experimentally from the data in Fig. 6, thus supporting the critical opalescence scenario.

4.3. Relevance to the mechanism of gel formation

As mentioned in the introduction, the question of the mechanism of RF gel formation remains unanswered. In the case of the nanostructured gels synthesized at higher pH, two different mechanisms are discussed in the literature that cannot be discriminated by SAXS (Gommes & Roberts, 2008). One possible mechanism is an aggregation process, by which colloidal particles aggregate to form space-filling clusters. The other mechanism is a microphase separation process, driven by the lowering of the polymer solubility in the course of the gel formation. The issue is not limited to RF gels, as several different mechanisms are also possible in inorganic gels (Gommes, Goderis, Pirard & Blacher, 2007).

Concerning the low-PH RF gels specifically, their microstructure lies in the micrometre range (see Fig. 1). Analyzing the phenomenology of their structure development would require static visible light scattering, which proved impossible because of multiple scattering. The present work therefore does not tell us anything either about the phenomenology of the structure development or about the morphology of the created structures. What the reported data do tell us, however, is what the driving force of the process is. The only possible explanation of critical fluctuations is a thermodynamic instability.

Critical fluctuations accompany any phase separation phenomenon. In other studies of reaction-induced phase separation in two different types of hybrid silica gels, a similar variation in the SAXS intensity was observed together with a -2 asymptotic exponent (Gommes *et al.*, 2004, 2005). The reason why critical fluctuations were not clearly identified in these studies is that the gels being formed were structured in the nanometre range, so that the SAXS signal of the structure was overlapping with that of the fluctuations. In the case of low-pH RF gels, the size of the structures being formed (about 5 μm, Fig. 1) is about two orders of magnitude larger than the upper resolution limit of SAXS (roughly 50 nm). This enables the unambiguous analysis of the scattering due to the critical fluctuations, almost unaffected by the scattering of the structure.

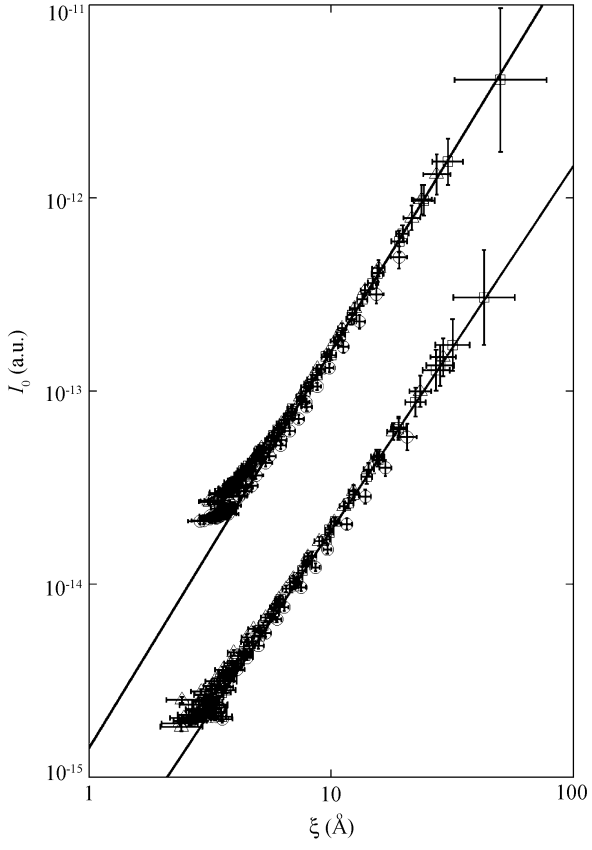

Figure 6
Relation between I_0 (proportional to osmotic compressibility χ) and ξ, before (bottom) and after (top) the critical time: pH = 2.7 (circles), pH = 3.0 (triangles) and pH = 3.7 (squares). The data after the critical time have been arbitrarily shifted vertically by a factor of ten, otherwise all points fall on the same power law with $I_0 \simeq \xi^2$.

5. Conclusions

The SAXS intensity measured during the formation of RF gels at low pH exhibits a non-monotonic intensity variation in the course of the gel formation, with an asymptotic scattering exponent of 2. These features result from the X-ray scattering by statistical fluctuations of polymer concentration, the amplitude of which is maximal close to the critical point of phase separation between the polymer and the solvent. The SAXS patterns are well described by the Orstein–Zernicke–Debye theory with the standard values of the critical exponents. The reason why critical fluctuations can be detected so clearly for RF gels at low pH is that the phase separation itself occurs on a length scale two orders of magnitude larger than the resolution of the SAXS, so that the intensities scattered by the structure and by the fluctuations do not overlap.

From a methodological point of view the present study shows how using SAXS to analyze the formation of a micrometre-sized structure – although not giving any information about the morphology of the structures being formed – can give a clear insight into the driving force of the process. The present observation of critical fluctuations points unambiguously to a thermodynamic instability of the polymerizing solution, and therefore to a reaction-induced phase separation process.

CJG and NJ are postdoctoral researchers of the Belgian National Fund for Scientific Research (FNRS); BG is a post-

electronic reprint

doctoral fellow of the Fund for Scientific Research Flanders (FWO–Vlaanderen). The authors thank Dr Wim Bras and Dr Florian Meneau (DUBBLE–CRG/ESRF) as well as Dr René Pirard (University of Liège) for their assistance in acquiring the *in situ* SAXS patterns. This work was supported by the National Fund for Scientific Research, Belgium, the Région Wallonne, Direction Générale des Technologies de la Recherche et de l'Energie, and the Interuniversity Attraction Poles Program, Belgian Science Policy P6/17.

References

Al-Muhtaseb, S. A. & Ritter, J. A. (2003). *Adv. Mater.* **15**, 101–114.
An, X., Xia, K.-Q., Shen, W. & Qiu, X.-L. (1999). *J. Chem. Phys.* **111**, 8298–8301.
Billmeyer, F. W. (1984). *Textbook of Polymer Science*, 3rd ed. New York: Wiley.
Brinker, C. J. & Scherer, G. W. (1990). *Sol-Gel Science: The Physics and Chemistry of Sol-Gel Processing*. San-Diego: Academic Press.
Burchard, W. (1977). *Macromolecules*, **10**, 919–927.
Gennes, P.-G. de (1979). *Scaling Concepts in Polymer Physics*. Ithaca: Cornell University Press.
Glatter, O. & Kratky, O. (1982). *Small-Angle X-ray Scattering*. New York: Academic Press.
Gommes, C. J., Blacher, S., Goderis, B. & Pirard, J.-P. (2005). *Nucl. Instrum. Methods Phys. Res. B*, **238**, 141–145.
Gommes, C. J., Blacher, S., Goderis, B., Pirard, R., Heinrichs, B., Alié, C. & Pirard, J.-P. (2004). *J. Phys. Chem. B*, **108**, 8983–8991.
Gommes, C. J., Goderis, B. & Pirard, J.-P. (2007). *J. Phys. Chem. C*, **111**, 11150–11156.
Gommes, C. J., Goderis, B., Pirard, J.-P. & Blacher, S. (2007). *J. Non-Cryst. Solids*, **353**, 2495–2499.
Gommes, C. J. & Roberts, A. P. (2008). *Phys. Rev. E*, **77**, 041409.
Goossens, S., Goderis, B. & Groeninckx, G. (2006). *Macromolecules*, **39**, 2953–2963.
Ishii, Y. & Ryan, A. J. (2000). *Macromolecules*, **33**, 158–166.
Job, N., Pirard, R., Marien, J. & Pirard, J.-P. (2004). *Carbon*, **42**, 619–628.
Nakanishi, K. (1997). *J. Porous Mater.* **4**, 67–112.
Olabisi, O., Robeson, L. M. & Shaw, M. T. (1979). *Polymer–Polymer Miscibility*. New York: Academic Press.
Pekala, R. W. (1989). *J. Mater. Sci.* **24**, 3221–3227.
Pekala, R. W. & Schaefer, D. W. (1993). *Macromolecules*, **26**, 5487–5493.
Sanchez, I. C. (1989). *J. Phys. Chem.* **93**, 6983–6991.
Schaefer, D. W., Pekala, R. W. & Beaucage, G. (1995). *J. Non-Cryst. Solids*, **186**, 159–167.
Sefcik, J. & McCormick, A. V. (1997). *Catal. Today*, **35**, 205–223.
Serrano Aroca, A., Monleón Pradas, M. & Gómez Ribelles, J. L. (2007). *Colloid Polym. Sci.* **285**, 753–760.
Stanley, H. E. (1971). *Introduction to Phase Transitions and Critical Phenomena*. Oxford: Clarendon Press.
Tanaka, T. (1981). *Sci. Am.* January, 124–138.
Yamamoto, T., Nishimura, T., Suzuki, T. & Tamon, H. (2001). *J. Non-Cryst. Solids*, **288**, 46–55.

electronic reprint